

Development and implementation of innovative higher order inverse polynomial method for tackling physical models in epidemiology



S. E. Fadugba^{a,*}, M. C. Kekana^b, N. Jeeva^c, I. Ibrahim^d

^aDepartment of Mathematics, Ekiti State University, Ado Ekiti, 360001, Nigeria.

^bDepartment of Mathematics, Tshwane University of Technology, Pretoria, South Africa.

^cPG and Research Department of Mathematics, The Madura College, Madurai, Tamil Nadu, India.

^dDepartment of Mathematics, Federal University, Dutse, Nigeria.

Abstract

This study introduces a new approach termed the Higher Order Inverse Polynomial Method (HOIPM) to tackle diverse model types. We analyze HOIPM's unique attributes and verify them through three illustrative scenarios. Additionally, we conduct a comparative assessment with the classical fourth-order Runge-Kutta method (RK4) to evaluate accuracy and computational efficiency. Real-world applications, such as predator-prey, SIR, and SEIR models, highlight HOIPM's effectiveness.

Keywords: Computing performance, convergence feature, error, precise value, veracity.

2020 MSC: 34A12, 65L05, 65L20, 65L70.

©2025 All rights reserved.

1. Introduction

As computational techniques advance, researchers continuously pursue innovative methods to improve accuracy, efficiency, and stability in addressing real-world problems. One-step and multistep methods are utilized in numerical analysis for approximating solutions to initial value problems [12, 25, 28]. In various scientific and engineering domains, selecting appropriate numerical methods and step sizes is crucial for obtaining dependable approximations to initial value problems. However, the ongoing aim of scholars is to devise numerical algorithms that surpass existing methodologies in accuracy, which is the primary objective of this investigation.

Several researchers have explored solutions to initial value problems (IVPs) in ordinary differential equations (ODEs) using both established and newly devised techniques, with further details provided in references [1, 3, 5, 6, 9–11, 13–19, 21, 23, 24, 27, 29], among others. The application of inverse polynomial methods for solving differential equations has been studied extensively, as evidenced by the work conducted by [2, 22], which introduced a fourth-stage inverse polynomial scheme. Fadugba et al. [8]

*Corresponding author

Email address: sunday.fadugba@eksu.edu.ng (S. E. Fadugba)

doi: [10.22436/jmcs.036.04.07](https://doi.org/10.22436/jmcs.036.04.07)

Received: 2024-05-04 Revised: 2024-05-29 Accepted: 2024-06-29

developed and analyzed the inverse polynomial scheme (ISM5) of order five for solving IVPs in ODEs, demonstrating its accuracy, efficiency, and superiority over RK5. Subsequently, a novel sixth-order inverse polynomial approach that surpasses the current RK4 method in addressing first-order IVPs with higher accuracy was introduced by [7]. The method was evaluated on several nonlinear physical models, with the proposed approach taking 3 to 5 seconds on the CPU.

This study investigates the development and application of a higher-order inverse polynomial method (HOIPM) for IVPs, discussing its theoretical foundations, implementations, and contributions to the field. In the ensuing sections, the derivation of the new HOIPM, its convergence and stability characteristics, and numerical examples are discussed. To demonstrate the accuracy of HOIPM, numerical experiments were conducted in this study and compared with the classical Runge-Kutta technique of order four (CRK4) and precise value (PV). Real-world problems are also addressed using HOIPM, with three models considered for this purpose. The prey-predator model elucidates the dynamics of biological systems where two species engage in interaction, one acting as the predator and the other as the prey [20]. The SIR model, a widely recognized epidemiological framework, is employed for examining the transmission dynamics of infectious diseases within a population. In this model, "SIR" represents the susceptible, infected, and recovered compartments, delineating the key population groups involved in disease spread and recovery [26]. Similarly, the SEIR model comprises susceptible, exposed, infected, and recovered compartments [4]. This serves as a suitable benchmark for comparison to demonstrate the new method's applicability, accuracy, and effectiveness in the context of precise value. The findings obtained will be further examined in subsequent sections, followed by the conclusion of the article.

2. Development of HOIPM

The development of HOIPM for the solution of

$$dy = \eta(x, y)dx, y(\beta) = y_0, \quad -\infty < y < \infty, \beta \leq x \leq \gamma,$$

is as follows. Consider the inverse interpolating polynomial

$$y_{n+1} = y_n \left[\sum_{j=0}^7 \zeta_j x_n^j \right]^{-1}, \quad (2.1)$$

where ζ_j 's are constants. From (2.1), one obtains

$$y_{n+1} = y_n [\zeta_0 x_n^0 + \zeta_1 x_n + \zeta_2 x_n^2 + \zeta_3 x_n^3 + \zeta_4 x_n^4 + \zeta_5 x_n^5 + \zeta_6 x_n^6 + \zeta_7 x_n^7]^{-1}. \quad (2.2)$$

Setting $\zeta_0 = 0$ and expanding (2.2) via binomial expansion, we obtain

$$\begin{aligned} y_{n+1} = y_n [& 1 - (\zeta_1 x_n + \zeta_2 x_n^2 + \zeta_3 x_n^3 + \zeta_4 x_n^4 + \zeta_5 x_n^5 + \zeta_6 x_n^6 + \zeta_7 x_n^7) \\ & + (\zeta_1 x_n + \zeta_2 x_n^2 + \zeta_3 x_n^3 + \zeta_4 x_n^4 + \zeta_5 x_n^5 + \zeta_6 x_n^6 + \zeta_7 x_n^7)^2 \\ & - (\zeta_1 x_n + \zeta_2 x_n^2 + \zeta_3 x_n^3 + \zeta_4 x_n^4 + \zeta_5 x_n^5 + \zeta_6 x_n^6 + \zeta_7 x_n^7)^3 \\ & + (\zeta_1 x_n + \zeta_2 x_n^2 + \zeta_3 x_n^3 + \zeta_4 x_n^4 + \zeta_5 x_n^5 + \zeta_6 x_n^6 + \zeta_7 x_n^7)^4 \\ & - (\zeta_1 x_n + \zeta_2 x_n^2 + \zeta_3 x_n^3 + \zeta_4 x_n^4 + \zeta_5 x_n^5 + \zeta_6 x_n^6 + \zeta_7 x_n^7)^5 \\ & + (\zeta_1 x_n + \zeta_2 x_n^2 + \zeta_3 x_n^3 + \zeta_4 x_n^4 + \zeta_5 x_n^5 + \zeta_6 x_n^6 + \zeta_7 x_n^7)^6 \\ & - (\zeta_1 x_n + \zeta_2 x_n^2 + \zeta_3 x_n^3 + \zeta_4 x_n^4 + \zeta_5 x_n^5 + \zeta_6 x_n^6 + \zeta_7 x_n^7)^7]. \end{aligned} \quad (2.3)$$

Rewriting the left-hand side (LHS) of equation (2.3) using Taylor's series expansion one obtains

$$\begin{aligned} & h \left[y'_n + \frac{h}{2!} y''_n + \frac{h^2}{3!} y'''_n + \frac{h^3}{4!} y^{iv}_n + \frac{h^4}{5!} y^v_n + \frac{h^5}{6!} y^{vi}_n + \frac{h^6}{7!} y^{vii}_n \right] \\ &= y_n [1 - (\zeta_1 x_n + \zeta_2 x_n^2 + \zeta_3 x_n^3 + \zeta_4 x_n^4 + \zeta_5 x_n^5 + \zeta_6 x_n^6 + \zeta_7 x_n^7) \\ &\quad + (\zeta_1 x_n + \zeta_2 x_n^2 + \zeta_3 x_n^3 + \zeta_4 x_n^4 + \zeta_5 x_n^5 + \zeta_6 x_n^6 + \zeta_7 x_n^7)^2 \\ &\quad - (\zeta_1 x_n + \zeta_2 x_n^2 + \zeta_3 x_n^3 + \zeta_4 x_n^4 + \zeta_5 x_n^5 + \zeta_6 x_n^6 + \zeta_7 x_n^7)^3 \\ &\quad + (\zeta_1 x_n + \zeta_2 x_n^2 + \zeta_3 x_n^3 + \zeta_4 x_n^4 + \zeta_5 x_n^5 + \zeta_6 x_n^6 + \zeta_7 x_n^7)^4 \\ &\quad - (\zeta_1 x_n + \zeta_2 x_n^2 + \zeta_3 x_n^3 + \zeta_4 x_n^4 + \zeta_5 x_n^5 + \zeta_6 x_n^6 + \zeta_7 x_n^7)^5 \\ &\quad + (\zeta_1 x_n + \zeta_2 x_n^2 + \zeta_3 x_n^3 + \zeta_4 x_n^4 + \zeta_5 x_n^5 + \zeta_6 x_n^6 + \zeta_7 x_n^7)^6 \\ &\quad - (\zeta_1 x_n + \zeta_2 x_n^2 + \zeta_3 x_n^3 + \zeta_4 x_n^4 + \zeta_5 x_n^5 + \zeta_6 x_n^6 + \zeta_7 x_n^7)^7]. \end{aligned} \quad (2.4)$$

By equating (2.4) term by term, one gets

$$\begin{aligned} \zeta_1 &= \frac{-hy'_n}{x_n y_n}, \\ \zeta_2 &= \frac{1}{2x_n^2 y_n^2} [2h^2(y'_n)^2 - h^2 y_n y''_n], \\ \zeta_3 &= \frac{1}{6x_n^3 y_n^3} [-h^3 y_n^2 y'''_n - 6h^3 (y'_n)^3 + 6h^3 y_n y'_n y''_n], \\ \zeta_4 &= \frac{1}{24x_n^4 y_n^4} [24h^4 (y'_n)^4 - 36h^4 y_n y_n'^2 y''_n + 8h^4 y_n^2 y'_n y'''_n - h^4 y_n^3 y_n'^v + 6h^4 (y_n)^2 (y''_n)^2], \\ \zeta_5 &= \frac{1}{120x_n^5 y_n^5} [-120h^5 (y'_n)^5 + 240h^5 y_n (y'_n)^3 y''_n - 180h^5 y_n^2 (y'_n)^2 y''_n \\ &\quad - 90h^5 y_n^2 (y'_n) (y''_n)^2 + 10h^5 y_n^3 (y'_n) y_n^{iv} + 20h^5 y_n^3 y''_n y'''_n - h^5 y_n^v], \\ \zeta_6 &= \frac{1}{720x_n^6 y_n^6} [-720h^6 (y'_n)^6 - 1800h^6 y'_n y_n y''_n + 480h^6 (y'_n)^3 y_n^5 + 1080h^6 (y'_n)^2 (y_n)^2 (y''_n)^2 \\ &\quad + 90h^6 (y_n)^3 (y''_n)^3 + 270h^6 (y'_n)^2 (y_n)^3 (y_n y_n^{iv}) (y''_n)^2 - 120h^6 (y'_n)^2 (y_n)^3 (y_n^{iv}) (y''_n)^2], \\ \zeta_7 &= \frac{1}{5040x_n^7 y_n^7} [-5040h^7 (y'_n)^7 - 840h^7 y_n (y'_n)^5 y''_n + 6720h^7 y_n^5 (y'_n)^4 \\ &\quad + 1260h^7 y_n^3 y'_n (y''_n)^3 + 2100h^7 y_n^3 y_n'^v (y'_n)^3 (y''_n)^2 + 15120h^7 y_n (y'_n)^3 (y''_n)^2 \\ &\quad - 25200h^7 y_n y'_n y''_n - 54h^7 y_n^2 (y'_n)^3 (y''_n)^2]. \end{aligned} \quad (2.5)$$

Substituting all equations in (2.5) into (2.2) and simplifying further, one obtains HOIPM

$$y_{n+1} = y_n \left\{ 1 - \omega_1 + \frac{\omega_2}{2y_n^2} + \frac{\omega_3}{6y_n^3} + \frac{\omega_4}{24y_n^4} + \frac{\omega_5}{120y_n^5} + \frac{\omega_6}{720y_n^6} + \frac{\omega_7}{5040y_n^7} \right\}^{-1} \quad (2.6)$$

with

$$\begin{aligned} \omega_1 &= \frac{hy'_n}{y_n}, \\ \omega_2 &= 2h^2 (y'_n)^2 - h^2 y_n y''_n, \\ \omega_3 &= -h^3 y_n^2 y'''_n - 6h^3 (y'_n)^3 + 6h^3 y_n y'_n y''_n \\ \omega_4 &= 24h^4 (y'_n)^4 - 36h^4 y_n y_n'^2 y''_n + 8h^4 y_n^2 y'_n y'''_n - h^4 y_n^3 y_n'^v + 6h^4 (y_n)^2 (y''_n)^2, \\ \omega_5 &= -120h^5 (y'_n)^5 + 240h^5 y_n - 90h^5 y_n^2 (y'_n) (y''_n)^2 (y'_n)^3 y''_n - 180h^5 y_n^2 (y'_n)^2 y''_n \end{aligned} \quad (2.7)$$

$$\begin{aligned}
& + 10h^5 y_n^3 (y_n') y_n^{iv} + 20h^5 y_n^3 y_n'' y_n''' - h^5 y_n^5, \\
\omega_6 = & -720h^6 (y_n')^6 - 1800h^6 y_n' y_n y_n'' + 480h^6 (y_n')^3 y_n^5 + 1080h^6 (y_n')^2 (y_n)^2 (y_n'')^2 \\
& + 90h^6 (y_n)^3 (y_n'')^3 + 270h^6 (y_n')^2 (y_n)^3 (y_n y_n^{iv}) (y_n'')^2 - 120h^6 (y_n')^2 (y_n)^3 (y_n') (y_n'')^2, \\
\omega_7 = & -5040h^7 (y_n')^7 - 840h^7 y_n (y_n')^5 y_n'' + 6720h^7 y_n^5 (y_n')^4 + 1260h^7 y_n^3 y_n' (y_n'')^3 \\
& + 2100h^7 y_n^3 y_n^{iv} (y_n')^3 (y_n'')^2 + 15120h^7 y_n (y_n')^3 (y_n'')^2 - 25200h^7 y_n y_n' y_n'' - 54h^7 y_n^2 (y_n')^3 (y_n'')^2.
\end{aligned}$$

3. Properties of HOIPM

The properties of HOIPM are analysed and examined as follows.

3.1. HOIPM's consistency

Theorem 3.1. HOIPM (2.6) employing an increment function $\alpha(x_n, y_n; h)$ is regarded as consistent if $\alpha(x_n, y_n; 0) = \eta(x_n, y_n)$.

Proof. Based on the definition of a general one-step method, it can be inferred that

$$\alpha(x_n, y_n; h) = \frac{y_{n+1} - y_n}{h}. \quad (3.1)$$

Using (2.6), (2.7), (3.1), and taking the limit of $\alpha(x_n, y_n; h)$ as $h \rightarrow 0$, we obtain

$$\lim_{h \rightarrow 0} \alpha(x_n, y_n; h) = \frac{5040 y_n^7 y_n'}{5040 y_n^7} = y_n' = \eta(x_n, y_n). \quad (3.2)$$

Equation (3.2) validates the consistency property of (2.6). Herein lies the culmination of our unique demonstration. \square

3.2. HOIPM's zero stability

Theorem 3.2. HOIPM (2.6) is deemed zero stable if its first characteristic polynomial $q(s) = e_1 s + e_0$ adheres to the following Dahlquist root conditions:

- (i) every root of $q(s)$ satisfy $|\omega| \leq 1$;
- (ii) several roots of $q(s)$ satisfy $|\omega| < 1$.

Proof. By (2.6), we have $e_1 = 1$ and $e_0 = -1$, yielding the characteristic polynomial:

$$q(s) = s - 1 \implies q(s) = 0 \implies s - 1 = 0 \implies s = 1.$$

Since the root of the first characteristic polynomial satisfies the Dahlquist root condition, it leads us to the conclusion that the Higher-Order Inverse Polynomial Method (HOIPM) exhibits zero stability. \square

3.3. HOIPM's stability property

Case 1: The absolute stability property of (2.6) is given in the following result.

Theorem 3.3. The stability of the derived method (2.6) is defined by its capability to guarantee that, for any initial error e_0 , there exists a constant η and $h > 0$ such that, when the general one-step scheme is utilized for an initial value problem with $h \in (0, h_0)$, the ensuing ultimate error e_n conforms to the specified inequalities $e_n \leq \mu e_0$ and $0 < \mu < 1$.

Proof. Using (2.2), the result follows from [7]. \square

Case 2: The linear stability property of HOIPM (2.6) is summarized in the following result.

Theorem 3.4. *Let's examine the linear test equation expressed as:*

$$y' = cy, \quad y(x_0) = y_0, \tag{3.3}$$

where c represents a constant. The stability polynomial associated with (2.6) is

$$p(z) = \sum_{q=0}^7 \frac{z^q}{\Gamma(q+1)}, \quad z = ch. \tag{3.4}$$

Proof. From (3.3), we have that

$$\begin{aligned} y'_n &= \eta_n = cy_n, & y''_n &= \eta_n^{(1)} = c^2y_n, & y'''_n &= \eta_n^{(2)} = c^3y_n, \\ y_n^{(iv)} &= \eta_n^{(3)} = c^4y_n, & y_n^{(v)} &= \eta_n^{(4)} = c^5y_n, & y_n^{(vi)} &= \eta_n^{(5)} = c^6y_n. \end{aligned}$$

Thus, (2.6) becomes

$$\frac{y_{n+1}}{y_n} = \left(1 + \frac{ch}{\Gamma(2)} + \frac{(ch)^2}{\Gamma(3)} + \frac{(ch)^3}{\Gamma(4)} + \frac{(ch)^4}{\Gamma(5)} + \frac{(ch)^5}{\Gamma(6)} + \frac{(ch)^6}{\Gamma(7)} \right). \tag{3.5}$$

Expressing z as ch in (3.5), (3.4) follows. □

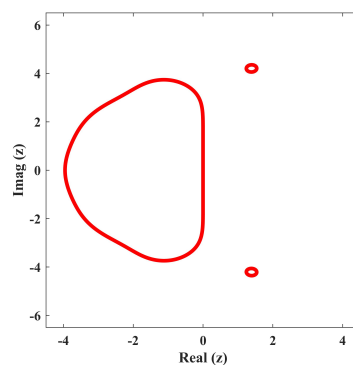


Figure 1: Linear stability region of HOIPM.

Figure 1 illustrates the linear stability region for HOIPM. Understanding this region is fundamental in numerical analysis, particularly for solving differential equations. The plot typically features the real part of the eigenvalues on the horizontal axis and the imaginary part on the vertical axis, representing the eigenvalues of the Jacobian matrix from the linearized differential equation. The shaded area in the plot indicates where the HOIPM remains stable. If the eigenvalues of the system lie within this area, the numerical solution will stay bounded and converge appropriately. The edges of this stability region are critical, marking the limit beyond which the method may become unstable, causing the solution to diverge.

3.4. HOIPM's convergence and Lipschitzian properties

Theorem 3.5. *Let \bar{b}_n denote a point situated within the interval bounded by y_n and \tilde{y}_n . Utilizing the mean value theorem establishes the convergence of (2.6). Moreover, the increment function of (2.6) demonstrates Lipschitzian properties for all (x_n, y_n) in the region D .*

Proof. By simplifying the derived method (2.6), the increment function is acquired in the following manner

$$\alpha(x_n, y_n; h) = \eta_n + I\eta_n^{(1)} + J\eta_n^{(2)} + K\eta_n^{(3)} + L\eta_n^{(4)} + M\eta_n^{(5)} + N\eta_n^{(6)}, \quad (3.6)$$

where

$$I = \frac{h}{2}, \quad J = \frac{h^2}{6}, \quad K = \frac{h^3}{24}, \quad L = \frac{h^4}{120}, \quad M = \frac{h^5}{720}, \quad N = \frac{h^6}{5040}.$$

Suppose

$$\alpha(x_n, \tilde{y}_n; h) = \tilde{\eta}_n + I\tilde{\eta}_n^{(1)} + J\tilde{\eta}_n^{(2)} + K\tilde{\eta}_n^{(3)} + L\tilde{\eta}_n^{(4)} + M\tilde{\eta}_n^{(5)} + N\tilde{\eta}_n^{(6)}. \quad (3.7)$$

Subtracting (3.7) from (3.6), one gets

$$\begin{aligned} \alpha(x_n, y_n; h) - \alpha(x_n, \tilde{y}_n; h) &= \eta_n - \tilde{\eta}_n + I[\eta_n^{(1)} - \tilde{\eta}_n^{(1)}] + J[\eta_n^{(2)} - \tilde{\eta}_n^{(2)}] + K[\eta_n^{(3)} - \tilde{\eta}_n^{(3)}] \\ &\quad + L[\eta_n^{(4)} - \tilde{\eta}_n^{(4)}] + M[\eta_n^{(5)} - \tilde{\eta}_n^{(5)}] + N[\eta_n^{(6)} - \tilde{\eta}_n^{(6)}]. \end{aligned}$$

Let \bar{b}_n denote a point situated within the interval bounded by y_n and \tilde{y}_n . Applying the mean value theorem, we have

$$\alpha(x_n, y_n; h) - \alpha(x_n, \tilde{y}_n; h) = [G + A_1H + A_2I + A_3J + A_4K + A_5L + A_6M + A_7N](y_n - \tilde{y}_n), \quad (3.8)$$

where $A_1, A_2, A_3, A_4, A_5, A_6, A_7$ are the least upper bound of $\frac{\partial \eta(x_n, \bar{b}_n)}{\partial y_n}$, $\frac{\partial \eta^{(1)}(x_n, \bar{b}_n)}{\partial y_n}$, $\frac{\partial \eta^{(2)}(x_n, \bar{b}_n)}{\partial y_n}$, $\frac{\partial \eta^{(3)}(x_n, \bar{b}_n)}{\partial y_n}$, $\frac{\partial \eta^{(4)}(x_n, \bar{b}_n)}{\partial y_n}$, $\frac{\partial \eta^{(5)}(x_n, \bar{b}_n)}{\partial y_n}$, $\frac{\partial \eta^{(6)}(x_n, \bar{b}_n)}{\partial y_n}$, respectively. Utilizing the norm operator on both sides of (3.8), results in

$$\|\alpha(x_n, y_n; h) - \alpha(x_n, \tilde{y}_n; h)\| \leq S \|y_n - \tilde{y}_n\|,$$

where the Lipschitz constant is represented as

$$S = \|G + A_1H + A_2I + A_3J + A_4K + A_5L + A_6M + A_7N\|.$$

As a result, the method (2.6) exhibits convergence and the increment function $\alpha(x_n, y_n; h)$ demonstrates Lipschitz continuity. \square

Remark 3.6. Additionally, it's worth noting that both consistency and stability act as essential and sufficient conditions for the convergence of a numerical method. With these criteria already fulfilled, we can confidently assert that the HOIPM method converges.

Remark 3.7. Employing the local truncation error (τ_n) for equation (2.6), we get

$$\tau_{n\{\text{HOIPM}\}} = \frac{h^8 f^{(viii)}(x_n, y_n)}{8!} + \dots$$

It is evident from the analysis that the method (2.6) exhibits accuracy up to the seventh order.

4. Applications and discussion of findings

The method's efficacy, precision, and efficiency were assessed through the examination of various non-linear physical models and real-world scenarios. Comparative analysis of the results involved evaluating the performance of HOIPM (2.6) alongside RK4 [19] and the precise value (PV) shall be presented. Also, the absolute deviation (ABE) for HOIPM (2.6) and RK4 will be calculated.

4.1. Applications

Consider the following nonlinear differential equations:

Example 4.1 ([7]). Consider non-linear physical model

$$\frac{dw}{dt} = aw - bw^2, \quad w(0) = 12, \quad a = 0.1, \quad b = 0.2, \quad (4.1)$$

with an exact value given by $w(t) = \frac{12ae^{at}}{a+12b(e^{at}-1)}$, where a represents the rate of virus transmission and

b denotes the rate of quarantine.

Example 4.2 ([20]). Consider prey-predator model

$$\frac{dn}{dt} = n(1-n) - \frac{np}{n+\alpha p}, \quad \frac{dp}{dt} = \delta p\left(\beta - \frac{p}{n}\right), \quad n(0) = 0.15, \quad p(0) = 0.05, \quad (4.2)$$

with the parameter values $\alpha = 0.1$, $\beta = 0.8$, and $\delta = 0.05$, where n is the prey population, p is the predator population, α represents the saturation effect of predation on the prey population, β is the predator death rate, and δ is the predator growth rate.

Example 4.3 ([26]). Consider Basic SIR model

$$\frac{dS}{dt} = -\beta SI, \quad \frac{dI}{dt} = \beta SI - \gamma I, \quad \frac{dR}{dt} = \gamma I, \quad S(0) = 0.95, \quad I(0) = 0.05, \quad R(0) = 0, \quad (4.3)$$

with the parameter values $\beta = 0.87$ and $\gamma = 0.08$, where S is the susceptible population, I is the infectious population, R is the recovered population, β is the transmission rate, indicating that the rate at which susceptible individuals become infected is relatively high, and γ is the recovery rate, indicating that once infected, individuals recover at a moderate rate.

Example 4.4 ([4]). Consider SEIR model

$$\begin{aligned} \frac{dS}{dt} &= \Lambda - \beta SI - \mu S + \rho R, & \frac{dE}{dt} &= \beta SI - (\alpha_1 + \mu)E, & \frac{dI}{dt} &= \alpha_1 E - (\alpha_2 + \mu + \delta)I + \phi I, & \frac{dR}{dt} &= \alpha_2 I - (\mu + \rho)R, \\ S(0) &= 0.95, & E(0) &= 0, & I(0) &= 0.05, & R(0) &= 0, \end{aligned} \quad (4.4)$$

with the parameter values $\Lambda = 0.1$, $\beta = 0.8$, $\mu = 0.05$, $\rho = 0.02$, $\alpha_1 = 0.1$, $\alpha_2 = 0.05$, $\delta = 0.02$, and $\phi = 0.03$, where S is the susceptible population, E is the exposed population, I is the infectious population, R is the recovered population, Λ is the recruitment rate into the susceptible population, β is the transmission rate, μ is the natural death rate, ρ is the rate of loss of immunity, α_1 is the rate at which exposed individuals become infectious, α_2 is the recovery rate from the infectious class, δ is the disease-induced death rate, and ϕ is the additional rate affecting the infectious population (e.g., re-infection rate).

Tables 1-4 depict the comparison of results between HOIPM (2.6) and RK4 for Examples 4.1-4.4, using a step size of $h = 0.1$ and various time increments (days).

Table 1: A comparison between HOIPM (2.6), RK4, and precise values for Example 4.1.

t	HOIPM	RK4	Exact
0	12.000000000000	12.000000000000	12.000000000000
3	1.723844908944	1.723852142785	1.723845440947
6	1.054728642126	1.054730652298	1.054728789660
9	0.819174191586	0.819175090162	0.819174257515
12	0.702883356414	0.702883846566	0.702883392372
15	0.635997221282	0.635997518595	0.635997243092
18	0.594114521820	0.594114714029	0.594114535919
21	0.566478560239	0.566478689695	0.566478569734
24	0.547607955559	0.547608045182	0.547607962133
27	0.534419430334	0.534419493571	0.534419434973
30	0.525051576462	0.525051621681	0.525051579778

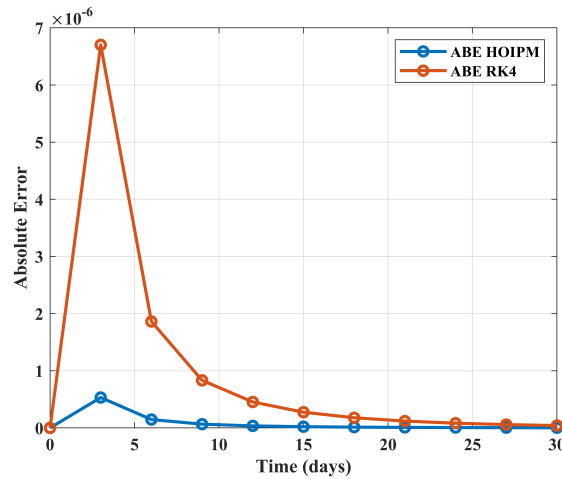


Figure 2: Graphical depiction of absolute deviation obtained via HOIPM and RK4 using Table 1.

Table 2: A comparison between HOIPM and RK4 for prey predator model Example 4.2.

t	HOIPM		RK4	
	n	p	n	p
0	0.1500000000	0.0500000000	0.1500000000	0.0500000000
3	0.6425963600	0.0551679199	0.6225934864	0.0549276507
6	0.9120790737	0.0618689578	0.9032579966	0.0612585662
9	0.9273564486	0.0693965689	0.9273299067	0.0683448681
12	0.9194758042	0.0777346549	0.9211169860	0.0761615140
15	0.9091384966	0.0869326431	0.9116200762	0.0847493321
18	0.8974211124	0.0970394861	0.9007985166	0.0941513043
21	0.8842435365	0.1080956455	0.8886837349	0.1044043727
24	0.8694410255	0.1201284620	0.8751473047	0.1155357281
27	0.8528254554	0.1331468318	0.8600341949	0.1275588543
30	0.8341858877	0.1471347777	0.8431712445	0.1404688108

Table 3: A comparison between HOIPM and RK4 for basic SIR model Example 4.3.

t	HOIPM			RK4		
	S	I	R	S	I	R
0	0.9500000000	0.0500000000	0.0000000000	0.9500000000	0.0500000000	0.0000000000
3	0.6427073340	0.3330711584	0.0242215077	0.6557745786	0.3210601152	0.0231653062
6	0.1519389018	0.7359391481	0.1121219501	0.1778593066	0.7174238672	0.1047168263
9	0.0208436593	0.7469043160	0.2322520248	0.0289574843	0.7528779182	0.2181645974
12	0.0033443944	0.6534662461	0.3431893595	0.0052233912	0.6695693852	0.3252072236
15	0.0006928563	0.5602710827	0.4390360610	0.0011677486	0.5799956946	0.4188365569
18	0.0001810900	0.4787702940	0.5210486160	0.0003202253	0.4999802025	0.4996995723
21	0.0000577782	0.4088397935	0.5911024283	0.0001050501	0.4305336829	0.5693612670
24	0.0000218441	0.3490603502	0.6509178057	0.0000402388	0.3706231410	0.6293366202
27	0.0000095400	0.2980049235	0.7019855365	0.0000176159	0.3190190491	0.6809633350
30	0.0000047099	0.2544119477	0.7455833423	0.0000086521	0.2745904756	0.7254008723

Table 4: A comparison between HOIPM and RK4 for basic SEIR model Example 4.4.

t	HOIPM				RK4			
	S	E	I	R	S	E	I	R
0	0.9500000000	0.0000000000	0.0500000000	0.0000000000	0.9500000000	0.0000000000	0.0500000000	0.0000000000
3	0.9935247386	0.0955559096	0.0517556909	0.0068780480	0.9913081359	0.0913664656	0.0514044939	0.0065642986
6	0.9944287510	0.1877083597	0.0776518015	0.0144507879	0.9949524540	0.1785665839	0.0748512906	0.0136957303
9	0.9180835119	0.3127472295	0.1267090225	0.0257994996	0.9300797546	0.2941784045	0.1191850276	0.0240766600
12	0.7595384361	0.4717443502	0.2032427878	0.0437789974	0.7894169194	0.4421492668	0.1881214853	0.0401759810
15	0.5584151334	0.6272285501	0.3053895624	0.0709747236	0.6016736066	0.5944532583	0.2811938050	0.0643011156
18	0.3834311816	0.7267587483	0.4181936159	0.1082767069	0.4250105997	0.7047961921	0.3874477418	0.0975561005
21	0.2736015287	0.7560251793	0.5203059309	0.1536512759	0.3026476823	0.7506379950	0.4887069881	0.1387431823
24	0.2184576082	0.7435713554	0.5984676006	0.2028758653	0.2352761499	0.7492517047	0.5709234695	0.1845967971
27	0.1930438908	0.7199707826	0.6517197711	0.2515959023	0.2022460987	0.7293029391	0.6302347409	0.2312765742
30	0.1812078381	0.6993626312	0.6855023861	0.2967271592	0.1863108520	0.7081582325	0.6698739631	0.2757051504

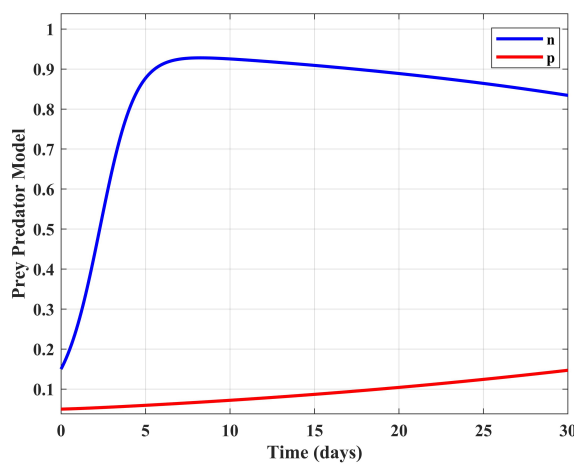


Figure 3: Graphical depiction of prey-predator model by HOIPM using Table 2.

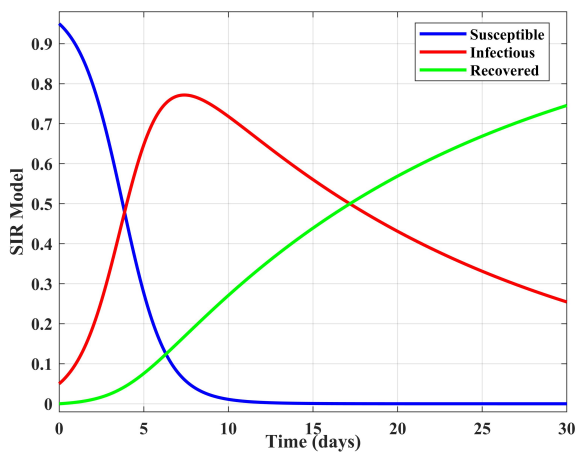


Figure 4: Graphical depiction of the basic SIR model by HOIPM using Table 3.

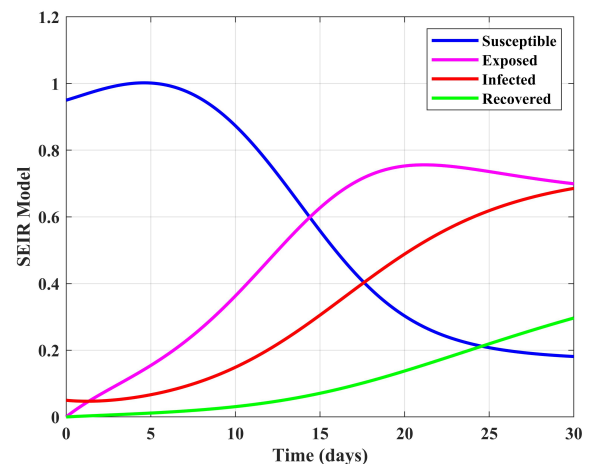


Figure 5: Graphical depiction of SEIR model by HOIPM using Table 4.

4.2. Discussion of Findings

The higher order inverse polynomial method (HOIPM) was utilized to compute numerical solutions for (4.1), showing strong agreement with exact values across different time intervals (t) using a step

size of $h = 0.1$, as depicted in Table 1. Figure 2 illustrates the Absolute Error Bounds (ABEs) obtained with HOIPM and RK4 for various t values, indicating HOIPM's closer alignment with the exact value curve compared to RK4. Additionally, HOIPM was applied to tackle the nonlinear differential equations found in prey-predator, SIR, and SEIR models, chosen for their complexity and suitability for evaluating HOIPM's effectiveness. Results indicate that HOIPM outperforms RK4 across these models. Table 2 compares HOIPM and RK4's performance on the prey predator model. Figure 3 presents a graphical representation of the results for the prey-predator model (4.2) from Table 2, obtained using the higher order implicit predictor method (HOIPM). The prey population $n(t)$ increases dramatically over time ($t > 5$), and predator population $p(t)$ slightly increases. Table 3 compares HOIPM and RK4's performance on the basic SIR model. Figure 4 depicts a graphic representation of the results of basic SIR model (4.3) from Table 3 using HOIPM. The susceptible population $S(t)$ declines dramatically ($t > 10$), while the recovery population $R(t)$ increases over the period of time. The infected population $I(t)$ increases at the beginning, but decreases over the time $t > 7$. Table 4 compares HOIPM and RK4's performance on the SEIR model. Figure 5 depicts a graphic representation of the the results of SEIR model (4.4) from Table 4 using HOIPM. The susceptible population $S(t)$ decreases over the time, but the exposed $E(t)$, infected $I(t)$, and recovered population $R(t)$ are increasing. HOIPM offers a more precise means of plotting real-life physical models like prey predator, SIR, SEIR, and so on.

5. Conclusions

The development and application of the proposed higher-order inverse polynomial method represent substantial contributions to the field of numerical analysis. By overcoming the limitations of conventional approaches related accuracy and stability, this method provides an alternative for researchers and practitioners seeking improved accuracy and stability in solving initial value problems (IVPs). Theoretical advancements and practical insights gained from its implementation contribute to a deeper understanding of numerical techniques for solving differential equations. While the higher-order inverse polynomial method shows promise, there are challenges and areas for further enhancement. Future research avenues may involve refining its stability analysis, expanding its applicability to a wider range of problems, and exploring parallel computing techniques for enhanced computational efficiency. The results demonstrate that HOIPM outperforms RK4 and converges more rapidly to the precise value as the step size (h) decreases, confirming its seventh-order accuracy. Notably, HOIPM exhibits greater efficiency compared to RK4, requiring less computational time and fewer gradient evaluations per iteration. Additionally, HOIPM is applied to real-world scenarios such as prey predator, SIR, and SEIR models based on empirical data.

References

- [1] M. Abdullahi, G. I. Danbaba, S. Abdulseed, *A New Multi-Block Super Class of BDF for Integrating First Order Stiff IVP of ODEs*, Current Res. Interdiscip. Stud., (2023), 1–13. 1
- [2] O. E. Abolarin, S. W. Akingbade, *Derivation and application of fourth stage inverse polynomial scheme to initial value problems*, IAENG Int. J. Appl. Math., **47** (2017), 459–464. 1
- [3] A. A. Adeniji, S. E. Fadugba, M. Y. Shatalov, *Comparative analysis of Lotka-Volterra type models with numerical methods using residuals in Mathematica*, Commun. Math. Biol. Neurosci., **2022** (2022), 1–17. 1
- [4] M. Al-Rahman El-Nor Osman, I. K. Adu, C. Yang, *A Simple SEIR Mathematical Model of Malaria Transmission*, Asian Res. J. Math., **7** (2017), 1–22. 1, 4.4
- [5] J. C. Butcher, *Numerical Methods for Ordinary Differential Equations*, John Wiley & Sons, Chichester, (2016). 1
- [6] S. O. Edeki, S. E. Fadugba, V. O. Udjor, O. P. Ogundile, D. A. Dosunmu, O. Ugbenu, N. Akindele, S. C. Zelibe, T. O. Kehinde, B. A. Jonah, *Approximate-analytical solutions of the quadratic Logistic differential model via SAM*, J. Phys.: Conf. Ser., **2199** (2022), 1–6. 1
- [7] S. E. Fadugba, I. Ibrahim, O. Adeyeye, A. A. Adeniji, M. C. Kekana, J. T. Okunlola, *A proposed sixth order inverse polynomial method for the solution of non-linear physical models*, J. Math. Comput. Sci., **32** (2024), 94–108. 1, 3.3, 4.1
- [8] S. E. Fadugba, V. J. Shaalini, A. A. Ibrahim, *Development and analysis of fifth stage inverse polynomial scheme for the solution of stiff linear and nonlinear ordinary differential equations*, J. Math. Comput. Sci., **10** (2020), 2926–2942. 1

- [9] I. Ghosh, M. S. H. Chowdhury, S. M. Aznam, *Numerical treatment on a chaos model of fluid flow using new iterative method*, J. Adv. Res. Fluid Mech. Therm. Sci., **96** (2022), 25–35. 1
- [10] I. Ghosh, M. M. Rashid, P. Ghosh, S. Mawa, R. Roy, M. M. Ahsan, K. D. Gupta, *Accurate Numerical Treatment on a Stochastic SIR Epidemic Model with Optimal Control Strategy*, Technologies, **10** (2022), 1–17.
- [11] I. Ghosh, M. M. Rashid, S. Mawa, *An evaluation of multispecies population dynamics models through numerical simulations using the new iterative method*, Healthcare Anal., **4** (2023), 1–11. 1
- [12] A. Hayat, S. S. Hasen, *Improved High order Euler Method for Numerical Solution of Initial value Time-Lag Differential Equations*, Iraqi J. Sci., **59** (2018), 383–388. 1
- [13] M. Heydari, G. B. Loghmani, S. M. Hosseini, *An improved piecewise variational iteration method for solving strongly nonlinear oscillators*, Comput. Appl. Math., **34** (2015), 215–249. 1
- [14] M. Heydari, G. B. Loghmani, S. M. Hosseini, *Exponential Bernstein functions: an effective tool for the solution of heat transfer of a micropolar fluid through a porous medium with radiation*, Comput. Appl. Math., **36** (2017), 647–675.
- [15] M. Heydari, G. B. Loghmani, S. M. Hosseini, S. M. Karbassi, *Application of hybrid functions for solving Duffingharmonic oscillator*, J. Differ. Equ., **2014** (2014), 9 pages.
- [16] M. Heydari, G. B. Loghmani, A.-M. Wazwaz, *A numerical approach for a class of astrophysics equations using piecewise spectral-variational iteration method*, Int. J. Numer. Methods Heat Fluid Flow, **27** (2017), 358–378.
- [17] M. H. Heydari, M. Razzaghi, *A numerical approach for a class of nonlinear optimal control problems with piecewise fractional derivative*, Chaos Solitons Fractals, **152** (2021), 9 pages.
- [18] M. Heydari, M. Razzaghi, D. Baleanu, *A numerical method based on the piecewise Jacobi functions for distributed-order fractional Schrödinger equation*, Commun. Nonlinear Sci. Numer. Simul., **116** (2023), 15 pages.
- [19] L. Lehmann (<https://math.stackexchange.com/users/115115/lutz-lehmann>), *Explanation and proof of the 4th order Runge-Kutta method*, URL (version: 2023-07-04). 1, 4
- [20] B. Li, S. Liu, J. Cui, J. Li, *A simple predator-prey population model with rich dynamics*, Appl. Sci., **6** (2016), 1–18. 1, 4.2
- [21] A. M. S. Mahdy, *A numerical method for solving the nonlinear equations of Emden-Fowler model*, J. Ocean Eng. Sci., (2022), 1–8. 1
- [22] R. B. Ogunrinde, *On a new inverse polynomial numerical scheme for the solution of initial value problems in ordinary differential equations*, Int. J. Aerosp. Mech. Eng., **9** (2015), 131–137. 1
- [23] R. B. Ogunrinde, R. R. Ogunrinde, S. E. Fadugba, *Analysis of the properties of a derived one-step numerical method of a transcendental function*, J. Interdiscip. Math., **24** (2021), 2201–2213. 1
- [24] S. Qureshi, A. Soomro, F. S. Emmanuel, E. Hincal, *A new family of L-stable block methods with relative measure of stability*, Int. J. Appl. Nonlinear Sci., **3** (2022), 197–222. 1
- [25] H. Ramos, G. Singh, V. Kanwar, S. Bhatia, *Solving first-order initial-value problems by using an explicit non-standard A-stable one-step method in variable step-size formulation*, Appl. Math. Comput., **268** (2015), 796–805. 1
- [26] H. S. Rodrigues, *Application of SIR epidemiological model: new trends*, Int. J. Appl. Math. Inform., **10** (2016), 92–97. 1, 4.3
- [27] J. V. Shaalini, A. E. K. Pushpam, *An application of exponential-polynomial single step method for viral model with delayed immune response*, Adv. Math.: Sci. J., **8** (2019), 154–161. 1
- [28] M. M. I. Sumon, M. Nurulhoque, *A Comparative Study of Numerical Methods for Solving Initial Value Problems (IVP) of Ordinary Differential Equations (ODE)*, Am. J. Appl. Math., **11** (2023), 106–118. 1
- [29] M. Tafakkori-Bafghi, G. B. Loghmani, M. Heydari, *Numerical solution of two-point nonlinear boundary value problems via Legendre-Picard iteration method*, Math. Comput. Simul., **199** (2022), 133–159. 1